Aperture-Coupled Stripline-to-Waveguide Transitions for Spatial Power Combining

Chris W. Hicks*, Alexander B. Yakovlev#, and Michael B. Steer+

*Naval Air Systems Command, RF Sensors Division 4.5.5, Patuxent River, MD 20670
#Department of Electrical Engineering, The University of Mississippi, University, MS 38677-1848
+Department of Electrical and Computer Engineering, North Carolina State University, Raleigh, NC 27695-7914

Abstract

A full-wave electromagnetic model is developed and verified for a waveguide transition consisting of slotted rectangular waveguides coupled to a strip line. This waveguide-based structure represents a portion of the planar spatial power combining amplifier array. The electromagnetic simulator is developed to analyze the stripline-to-slot transitions operating in a waveguide-based environment in the X-band. The simulator is based on the method of moments (MoM) discretization of the coupled system of integral equations with the piecewise sinusodial testing and basis functions in the electric and magnetic surface current density expansions. Electric and magnetic dyadic Green's functions used in this integral equation formulation are developed for an infinite rectangular waveguide in the form of partial expansion over the complete system of eigenfunctions of a transverse Laplacian operator. Numerical results are obtained and compared with a commercial microwave simulator for a few representative structures, including various configurations and planar arrays of slotted waveguide modules coupled to a strip line.

I. Introduction

Military and civilian applications require sizable power at microwave and millimeter-wave frequencies. Medium to high power levels are needed for applications such as communications, active missile seekers, radar, and millimeter-wave imaging. To meet this need, klystrons, traveling-wave tubes, and gridded tubes are heavily utilized to generate medium to high power. However, tubes are bulky, costly, require high operating voltages, and have a short lifetime. As an alternative, solid-state devices offer several advantages such as, lightweight, smaller size, wider bandwidths, and lower operating voltages. These advantages lead to lower cost because systems can be constructed using planar fabrication techniques. However, as the frequency increases, the output power of solid-state devices decreases due to their small physical size. Therefore, to achieve sizable power levels that compete with those generated by vacuum tubes, several solid-state devices can be combined in an array. Conventional power combiners are effectively limited in the number of devices that can be combined. To overcome these limitations and produce high power levels at microwave and millimeter-wave frequencies, in a past few years there has been a considerable activity in developing spatial power combining systems [1], [2], [3]. The output power of individual solid-state devices in a planar array is combined to produce moderate-to-high power levels. It is desirable to utilize a single solid-state amplifier, however, as frequency increases, the output power levels become low due to the $1/f^2$ fall-off of available power [4]. By utilizing power combining techniques light-weight, reliable, and low cost amplifiers and oscillators can be potentially designed to meet the demand of military and civilian applications.

Fundamental understanding of spatial power combining systems has primarily been done by experimental investigation. Several experimental free space and dielectric quasi-optical power combiners and waveguide spatial power combiners have been successful at demonstrating the fundamental concept of generating usable output power levels using spatial and quasi-optical techniques. Although great strides have been

1054-4887 © 2003 ACES

made, to date, quasi-optical/spatial power combining systems have not yet out performed conventional power combiners. In order to capture the full potential of quasi-optical/spatial systems to generate high power levels, numerical modeling and computer aid engineering tools are needed to fully understand these systems [5]. The development of computer models helps to reduce the cost and time associated with experimental work, and computer models assist with designing efficient quasi-optical/spatial power combining systems. Modeling a quasi-optical/spatial power combining system is complex and challenging. There are several major system components that must be modeled such as, the input and output sources, which are typically waveguide horns with optical lenses inside, the input and output antennas with associated transmission lines and control components, and the active integrated amplifier circuitry.

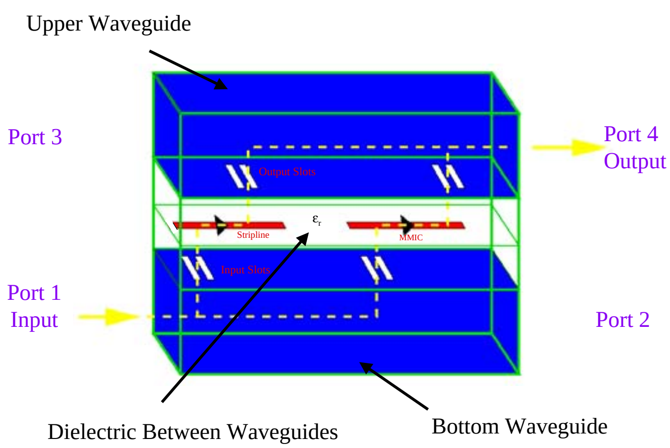

Fig. 1. Aperture-coupled stripline-to-waveguide transition.

In this paper, an electromagnetic modeling environment is developed for an aperture-coupled stripline-to-waveguide transition (with geometry shown in Fig. 1). This transition is the fundamental building block for two-dimensional spatial power combining amplifier arrays shown in Fig. 2 and, in turn, for the planar quasi-optical power combining systems. The transition consists of three infinite aperture-coupled rectangular waveguides. The lower slots (apertures) are located on the surface between the lower and middle waveguides, and the upper slots are located on the surface between the middle and upper waveguides. The strips are located inside of the middle waveguide region. The objective of stripline-to-waveguide transition is to efficiently couple energy from the lower waveguide to the upper waveguide. An incident electromagnetic field is illuminated at the input port of the lower waveguide. This signal travels into the lower waveguide and induces magnetic currents on the lower slots where the slots scatter energy into the lower, middle, and upper waveguides. In the middle waveguide region the scattered fields induce electric currents and standing waves along the strips. The scattered energy from the strips along with the scattered energy from the lower slots induce magnetic currents in the upper slots. The magnetic currents in the upper slots cause scattered fields back into the middle waveguide and into the upper waveguide region. Optimum performance is achieved by varying the distance between the slots, adjusting the slot dimensions, rotating the slots, or varying the stripline dimensions.

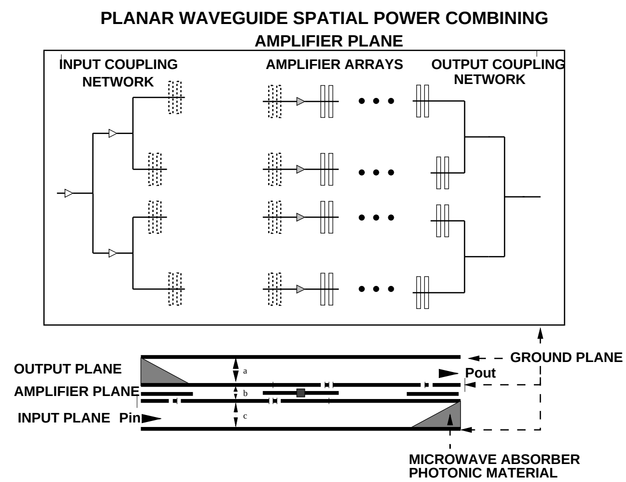

Fig. 2. Aperture-coupled planar waveguide amplifier array.

A full-wave electromagnetic model is developed for a structure that couples a waveguide to a stripline through a set of slots and from the stripline through another set of slots into a second waveguide. The system modeling is based on an integral equation formulation for the induced electric and magnetic surface current densities resulting in a coupled set of integral equations discretized via the method of moments (MoM). The scattered electric and magnetic fields are expressed in terms of dyadic Green's functions and the electric and magnetic surface currents. Electric and magnetic dyadic Green's functions are developed for an infinite rectangular waveguide in the form of partial expansion over the complete system of eigenfunctions of a transverse Laplacian operator. The surface currents are discretized by overlapping piecewise sinusodial subdomain basis functions in order to accurately model narrow longitudinal strips and transverse slots. In this formulation, a MoM matrix includes all possible self and mutual coupling effects between the slots and strips. The transition is excited with the TE_{10} dominant waveguide mode, and the scattering parameters are calculated from the forward and backward coupling coefficients in the waveguide regions.

Numerical results of the scattering characteristics are obtained and compared with a commercial microwave simulator for a few representative structures, including a single slot-strip-slot waveguide transition, multiple slot-strip-slot waveguide transitions, and planar arrays of slotted waveguide modules coupled to strip lines.

II. Theory

A general electromagnetic formulation for a closed-boundary waveguiding structure containing arbitrarily shaped apertures and conducting strips (see Fig. 3) is presented in this section. This structure is a general building block of the aperture-coupled stripline-to-waveguide transition shown in Fig. 1. The formulation is based on the integral representation of incident and scattered electric and magnetic fields in terms of dyadic Green's functions [6], [7]. Dyadic Green's functions represent the electric and magnetic fields at an observation point inside a volume due to an arbitrarily oriented point source. Fig. 3 shows an arbitrary volume V enclosed by the surface $\tilde{S} = S \cup S_m$, where S represents an electric-type boundary surface and S_m represents the surface of apertures (magnetic-type surface). The volume V encloses an impressed electric volume current source $\bar{J}_{imp} \subset V_{imp}$ and an electric current source $\bar{J}_{ind}$ induced on the surface of conducting strips S_e (electric-type surface).

The integral representations for the total electric and magnetic fields in volume V due to the impressed and induced currents are obtained as follows

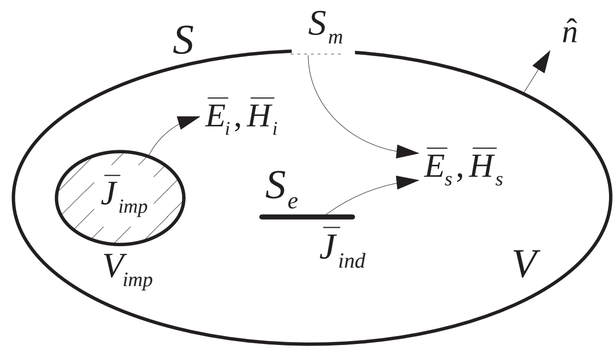

Fig. 3. Geometry of a closed-boundary waveguiding structure containing apertures and conducting strips in the presence of an impressed electric current source.

$$\begin{aligned}\bar{E}(\vec{r}) = -j\omega\mu \int_{V_{imp}} \bar{\bar{G}}_{EJ}(\vec{r},\vec{r}\,') \cdot \bar{J}_{imp}(\vec{r}\,')dV' \\ -j\omega\mu \int_{S_e} \bar{\bar{G}}_{EJ}(\vec{r},\vec{r}\,') \cdot \bar{J}_{ind}(\vec{r}\,')dS' \\ - \int_{S_m} \bar{\bar{G}}_{EM}(\vec{r},\vec{r}\,') \cdot \bar{M}(\vec{r}\,')dS' \quad (1)\end{aligned}$$

$$\begin{aligned}\bar{H}(\vec{r}) = \int_{V_{imp}} \bar{\bar{G}}_{HJ}(\vec{r},\vec{r}\,') \cdot \bar{J}_{imp}(\vec{r}\,')dV' \\ + \int_{S_e} \bar{\bar{G}}_{HJ}(\vec{r},\vec{r}\,') \cdot \bar{J}_{ind}(\vec{r}\,')dS' \\ -j\omega\epsilon \int_{S_m} \bar{\bar{G}}_{HM}(\vec{r},\vec{r}\,') \cdot \bar{M}(\vec{r}\,')dS' \quad (2)\end{aligned}$$

where

$$\bar{\bar{G}}_{HJ}(\vec{r},\vec{r}\,') = \nabla\times \bar{\bar{G}}_{EJ}(\vec{r},\vec{r}\,'), \quad (3)$$

$$\bar{\bar{G}}_{EM}(\vec{r},\vec{r}\,') = \nabla\times \bar{\bar{G}}_{HM}(\vec{r},\vec{r}\,'). \quad (4)$$

Here, the electric-electric dyadic Green's function, $\bar{\bar{G}}_{EJ}(\vec{r},\vec{r}\,')$, relates the electric field in volume V enclosed by surface $\tilde{S}$ to the impressed electric current source $\bar{J}_{imp}(\vec{r}) \in V_{imp}$ and the induced electric surface current $\bar{J}_{ind}(\vec{r}) \in S_e$; the electric-magnetic dyadic Green's function, $\bar{\bar{G}}_{EM}(\vec{r},\vec{r}\,')$, relates the electric field in the volume V to the equivalent magnetic surface current $\bar{M}(\vec{r}) \in S_m$; the magnetic-magnetic dyadic Green's function, $\bar{\bar{G}}_{HM}(\vec{r},\vec{r}\,')$, relates the magnetic field in the volume V to the equivalent magnetic surface current $\bar{M}(\vec{r}) \in S_m$, and the magnetic-electric dyadic Green's function, $\bar{\bar{G}}_{HJ}(\vec{r},\vec{r}\,')$, relates the magnetic field in the volume V to the impressed electric current source

$\bar{J}_{imp}(\vec{r}) \in V_{imp}$ and the induced electric surface current $\bar{J}_{ind}(\vec{r}) \in S_e$. These electric and magnetic dyadic Green's functions are developed for an infinite rectangular waveguide in the form of partial expansion over the complete system of eigenfunctions of a transverse Laplacian operator [8].

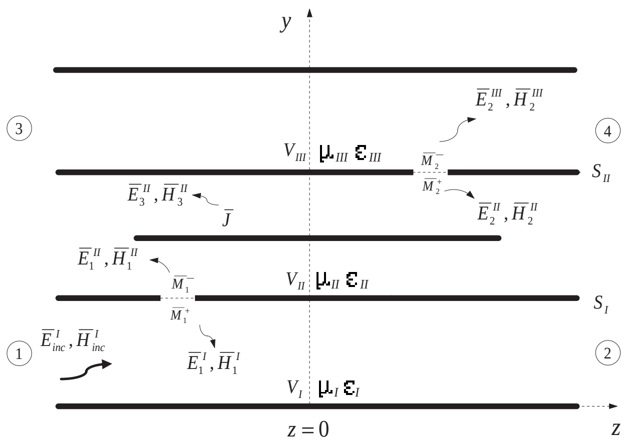

Fig. 4. Field analysis in terms of incident and scattered electric and magnetic fields due to induced electric and magnetic surface currents in the aperture-coupled stripline-to-waveguide transition.

The integral equation formulation discussed above was applied for the analysis of a structure that couples the lower waveguide (region V_I) to the stripline (region V_{II}) through a set of slots and from the stripline through another set of slots into the upper waveguide (region V_{III}) (Fig. 4). The geometry shown in Fig. 4 is a unit cell of a general topology of the aperture-coupled stripline-to-waveguide transition (Fig. 1). Fig. 4 shows a field analysis in terms of incident and scattered electric and magnetic fields in three different regions due to induced electric and magnetic surface currents. A coupled system of equations is obtained by imposing a continuity of tangential magnetic fields across the surfaces of lower and upper slots, S_1 and S_2, respectively, and an electric-field boundary condition on the surface of the strip, S_3,

$$\hat{y} \times \bar{H}_{inc}^{I}(\vec{r}) = \hat{y} \times [\bar{H}_1^{II}(\vec{r}) - \bar{H}_1^{I}(\vec{r}) + \bar{H}_2^{II}(\vec{r}) + \bar{H}_3^{II}(\vec{r})], \quad \vec{r} \in S_1 \tag{5}$$

$$0 = \hat{y} \times [\bar{H}_1^{II}(\vec{r}) + \bar{H}_2^{II}(\vec{r}) - \bar{H}_2^{III}(\vec{r}) + \bar{H}_3^{II}(\vec{r})], \quad \vec{r} \in S_2 \tag{6}$$

$$0 = \hat{y} \times [\bar{E}_1^{II}(\vec{r}) + \bar{E}_2^{II}(\vec{r}) + \bar{E}_3^{II}(\vec{r})], \quad \vec{r} \in S_3 \tag{7}$$

or it can be written in the integral form in terms of corresponding dyadic Green's functions and impressed and induced surface current densities

$$\begin{aligned} \hat{y} \times \bar{H}_{inc}^{I}(\vec{r}) = & \\ \hat{y} \times [j\omega\epsilon_{II} & \int_{S_1} \overline{\overline{G}}{}^{II}_{HM}(\vec{r}, \vec{r}\,') \cdot \bar{M}_1(\vec{r}\,') dS' \\ & - j\omega\epsilon_I \int_{S_1} \overline{\overline{G}}{}^{I}_{HM}(\vec{r}, \vec{r}\,') \cdot \bar{M}_1(\vec{r}\,') dS' \\ & - j\omega\epsilon_{II} \int_{S_2} \overline{\overline{G}}{}^{II}_{HM}(\vec{r}, \vec{r}\,') \cdot \bar{M}_2(\vec{r}\,') dS' \\ & + \int_{S_3} \overline{\overline{G}}{}^{II}_{HJ}(\vec{r}, \vec{r}\,') \cdot \bar{J}(\vec{r}\,') dS'], \quad \vec{r} \in S_1 \end{aligned} \tag{8}$$

$$\begin{aligned} 0 = \hat{y} \times [j\omega\epsilon_{II} & \int_{S_1} \overline{\overline{G}}{}^{II}_{HM}(\vec{r}, \vec{r}\,') \cdot \bar{M}_1(\vec{r}\,') dS' \\ & - j\omega\epsilon_{II} \int_{S_2} \overline{\overline{G}}{}^{II}_{HM}(\vec{r}, \vec{r}\,') \cdot \bar{M}_2(\vec{r}\,') dS' \\ & + j\omega\epsilon_{III} \int_{S_2} \overline{\overline{G}}{}^{III}_{HM}(\vec{r}, \vec{r}\,') \cdot \bar{M}_2(\vec{r}\,') dS' \\ & + \int_{S_3} \overline{\overline{G}}{}^{II}_{HJ}(\vec{r}, \vec{r}\,') \cdot \bar{J}(\vec{r}\,') dS'], \quad \vec{r} \in S_2 \end{aligned} \tag{9}$$

$$\begin{aligned} 0 = \hat{y} \times [& \int_{S_1} \overline{\overline{G}}{}^{II}_{EM}(\vec{r}, \vec{r}\,') \cdot \bar{M}_1(\vec{r}\,') dS' \\ & + \int_{S_2} \overline{\overline{G}}{}^{II}_{EM}(\vec{r}, \vec{r}\,') \cdot \bar{M}_2(\vec{r}\,') dS' \\ + j\omega\mu_{II} & \int_{S_3} \overline{\overline{G}}{}^{II}_{EJ}(\vec{r}, \vec{r}\,') \cdot \bar{J}(\vec{r}\,') dS'], \quad \vec{r} \in S_3. \end{aligned} \tag{10}$$

Here, $\bar{H}_{inc}^{I}(\vec{r})$ is the incident magnetic field generated in the lower waveguide; $\bar{M}_1(\vec{r}\,')$ and $\bar{M}_2(\vec{r}\,')$ are the equivalent magnetic surface currents induced on the surfaces of the lower and upper slots, S_1 and S_2, respectively; $\bar{J}(\vec{r}\,')$ is the electric surface current induced on the surface of the strip, S_3; $\overline{\overline{G}}_{HM}(\vec{r}, \vec{r}\,')$, $\overline{\overline{G}}_{HJ}(\vec{r}, \vec{r}\,')$, $\overline{\overline{G}}_{EM}(\vec{r}, \vec{r}\,')$, and $\overline{\overline{G}}_{EJ}(\vec{r}, \vec{r}\,')$ are the electric and magnetic Green's dyadics of the corresponding waveguides (regions V_I, V_{II}, and V_{III}). The surface currents are discretized by overlapping piecewise sinusodial subdomain basis functions. In this formulation, a MoM matrix includes all possible self and mutual coupling effects between the slots and strips. The transition is excited with the TE_{10} dominant waveguide mode and the scattering parameters are calculated from the forward and backward coupling coefficients in the waveguide regions. The details of the method of moments discretization technique of the slotted waveguide transitions and dyadic Green's functions applied in this formulation can be found in [8].

III. Numerical Results and Discussions

Numerical results of the scattering characteristics were obtained and compared with a commercial microwave simulator for a few representative structures shown in Fig. 5, including a single slot-strip-slot waveguide and multiple slot-strip-slot waveguide transitions. Also, planar arrays of slotted waveguide modules coupled to a strip line (with geometries shown in Figs. 8 and 10) are investigated.

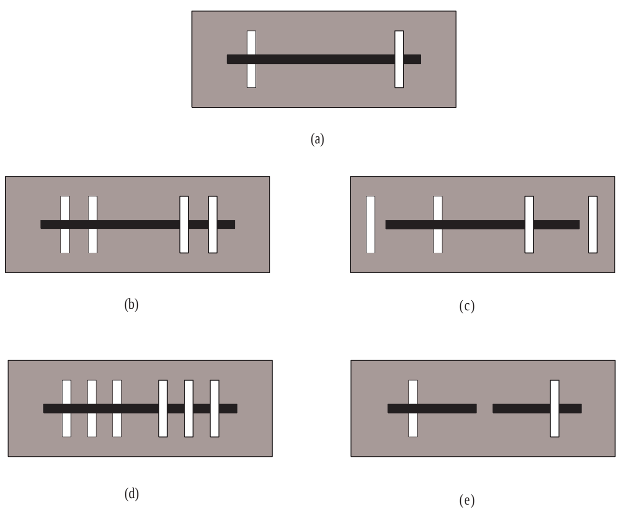

Fig. 5. Top view: (a) one lower slot, one strip, and one upper slot; (b) two lower slots, one strip, and two upper slots; (c) same as (b) but one lower slot and one upper slot are offset, (d) three lower slots, one strip, and three upper slots; and (e) one lower slot, two strips, and one upper slot.

Here we present numerical results of the scattering characteristics for the examples of the double slot-strip-slot waveguide transition with two shifted slots (case (c) in Fig. 5) and two strips coupled to two slots (case (e) in Fig. 5). In both examples, the upper and lower X-band waveguide dimensions are 22.86 mm × 10.16 mm, $\varepsilon_I = \varepsilon_{III} = 1.0$, while the middle waveguide dimensions are 22.86 mm × 1.5748 mm (62 mils), and $\varepsilon_{II} = 1.0$. In the case shown in Fig. 5(c), the spacing between the lower and upper slots is 19 mm, while the inter-spacing between the two lower slots and two upper slots is 10 mm. The length of the strip is 30 mm, the width of the strip is 1 mm, the length of the slots is 13 mm, and the width of the slots is 1 mm. The reflection coefficient S_{11} and the coupling coefficient S_{41} computed using the MoM technique presented here and the HFSS commercial program are compared in Fig. 6. The coupling of -8.6 dB occurs at approximately 9.2 GHz.

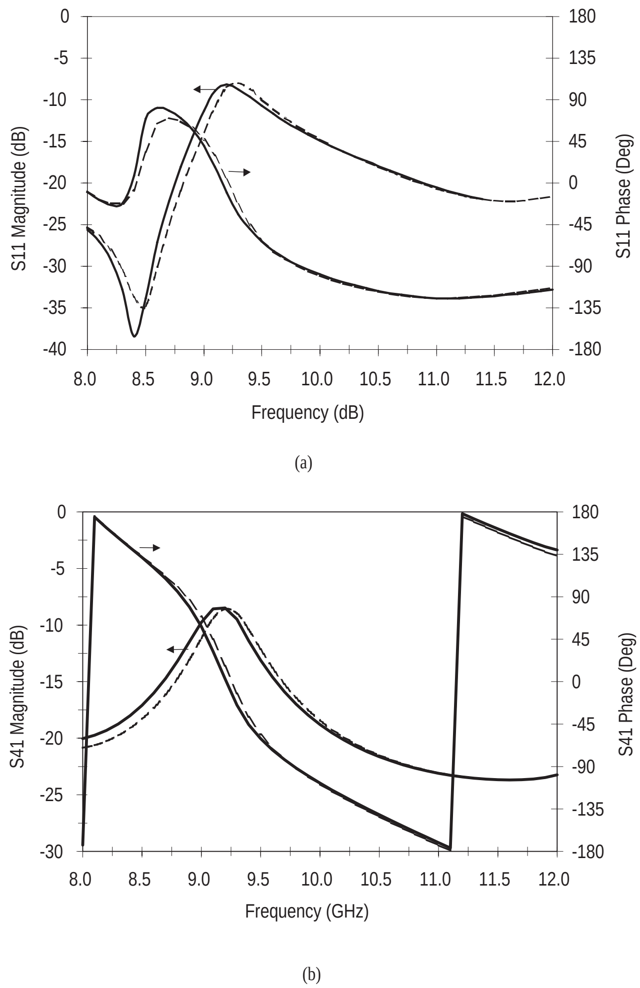

Fig. 6. MoM (solid line) and HFSS (dashed line) comparison for the scattering parameters (reflection and coupling coefficients) for the double slot-strip-slot waveguide transition with two offset slots. Magnitude and phase: (a) S_{11} and (b) S_{41}.

In the second example with geometry shown in Fig. 5(e), the longitudinal strip is divided into two strips

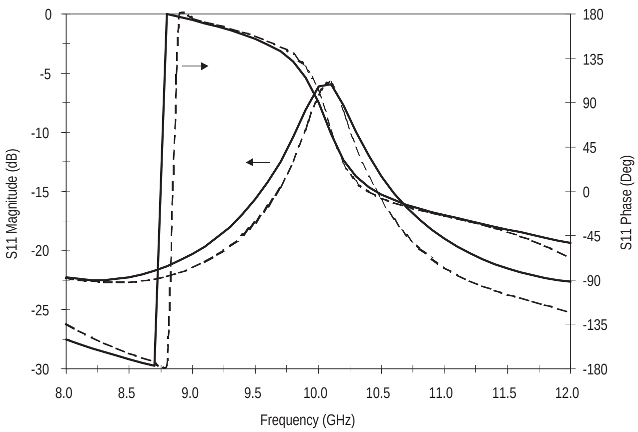

(a)

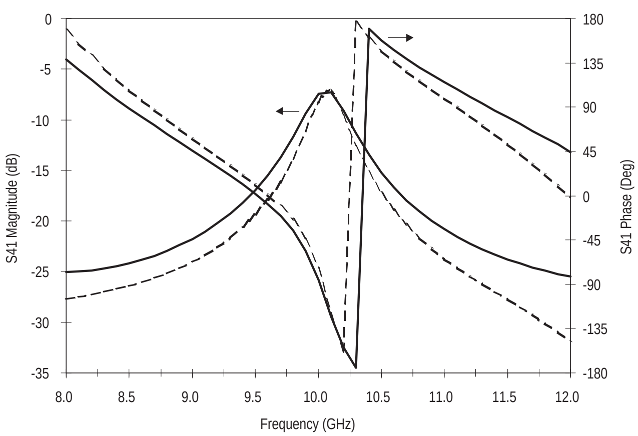

(b)

Fig. 7. MoM (solid line) and HFSS (dashed line) comparison of the scattering parameters for one lower slot, two strips, and one upper slot waveguide transition. Magnitude and phase: (a) S_{11} and (b) S_{41}.

each 10 mm in length. The length of the lower and upper slots is changed to 15 mm. In the method of moments program, the slots and strips are discretized in 1 mm cells. Both scattering parameters peak at 10 GHz (Fig. 7), and both magnitudes of S_{11} and S_{41} reach a peak value of approximately -5.5 dB and -7.2 dB, respectively.

Fig. 8 shows the geometry of the 1 $\times$ 2 waveguide coupler array which consists of 2 transitions in series shown in Fig. 5(a). Transitions are separated by 40

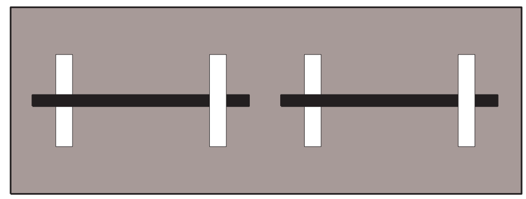

Fig. 8. Top view of the slotted 1 $\times$ 2 waveguide array with a unit cell shown in Fig. 5(a) consisting of one lower slot, one strip, and one upper slot.

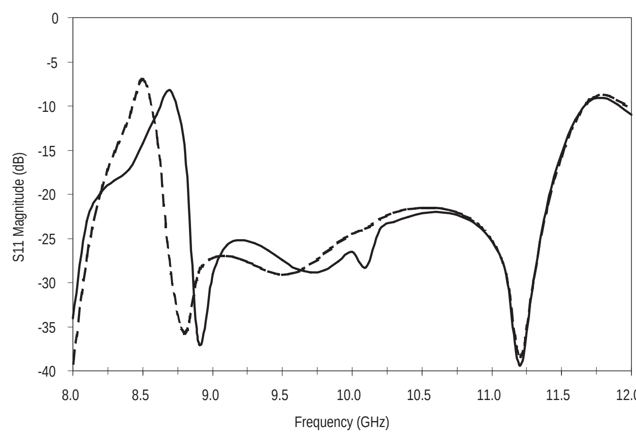

(a)

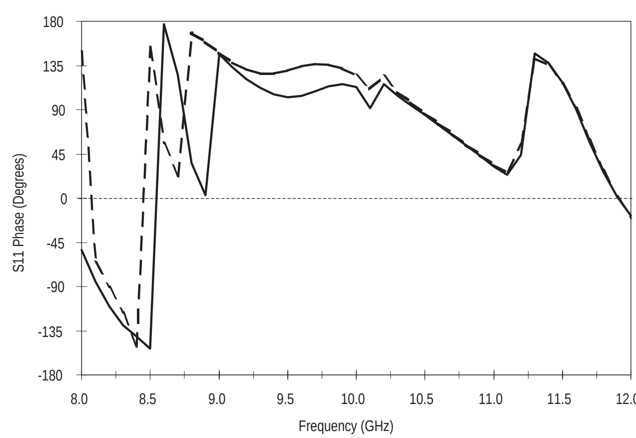

(b)

Fig. 9. MoM (solid line) and HFSS (dashed line) comparison of S_{11} for the 1 $\times$ 2 one lower slot, one strip, and one upper slot waveguide coupler array. (a) Magnitude and (b) phase.

mm with respect to the center, the waveguide length is 90 mm, and $\varepsilon_I = \varepsilon_{II} = \varepsilon_{III} = 1.0$.

Fig. 9 compares the MoM simulations and HFSS results for the magnitude and phase of the reflection coefficient S_{11}. The maximum and minimum values, -8.3 dB and -39.5 dB, of the reflection coefficient occur at 8.7 GHz and 11.2 GHz, respectively.

Fig. 10 shows the 2 × 2 slotted waveguide array which consists of four transitions with the geometry of a unit cell shown in Fig. 5(a). The 2 × 2 array represents two waveguide couplers separated by a distance of 23 mm. The length and width of the slots are 13 mm × 1 mm, and the length and width of the strip are 30 mm × 1 mm, respectively. Both the lower and upper waveguide width and height dimensions are 46.0 mm × 10.16 mm and $\varepsilon_I = \varepsilon_{III} = 1.0$. The middle waveguide dimensions are 46.0 mm × 1.5 mm and $\varepsilon_{II} = 2.2$.

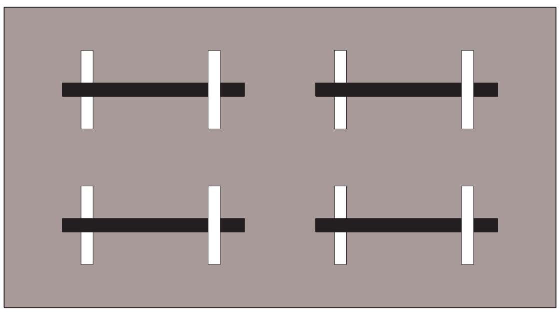

Fig. 10. Top view of a 2 × 2 one lower slot, one strip, and one upper slot waveguide array.

Fig. 11 shows the MoM simulations for the magnitude and phase of S_{11} for the 2 × 2 waveguide array. A total of $m = n = 125$ modes were utilized to simulate the array, and the cell size of slots and strips were discretized into 1 mm increments. The minimum value of -32.4 dB of S_{11} occurs at approximately 9.75 GHz.

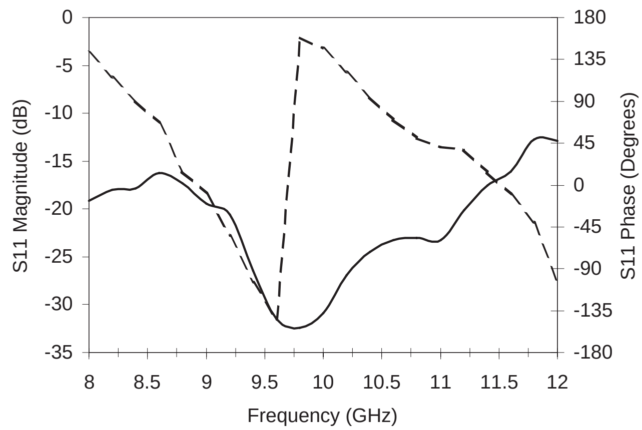

Fig. 11. MoM simulation of S_{11} for a 2 × 2 one lower slot, one strip, and one upper slot waveguide array. (a) Magnitude (solid line) and (b) phase (dashed line).

IV. Conclusion

In this paper we presented the analysis of aperture-coupled stripline-to-waveguide transitions used in planar spatial power combining systems. The method of analysis is based on the integral equation formulation for the unknown electric and magnetic surface currents with electric and magnetic dyadic Green's functions of infinite rectangular waveguide. The method of moments discretization with piecewise sinusoidal testing and basis functions reduces a coupled set of integral equations to a matrix equation. Numerical results obtained for the scattering parameters of various slot-strip-slot waveguide transitions and arrays compare well with the results calculated by the Finite Element Method commercial program (HFSS).

References

[1] P. F. Goldsmith, "Quasi-optical techiques at millimeter and sub-millimeter wavelenghs," in *Infrared and Millimeter Waves,* K. J. Button (Ed.), New York: Academic Press, Vol. 6, pp. 277–343, 1982.

[2] L. Wandinger and V. Nalbandian, "Millimeter-wave power-combining using quasi-optical techniques," *IEEE Trans. on Microwave Theory and Techn.,* Vol. 31, pp. 189–193, February 1983.

[3] R. A. York, Z. B. Popović *Active and Quasi-Optical Arrays for Solid-State Power Combining*, John Wiley & Sons, New York, New York, 1997.

[4] J. C. Wiltse and J. W. Mink, "Quasi-optical power combining of solid-state sources," *Microwave Journal,* pp. 144–156, February 1992.

[5] M. B. Steer, J. F. Harvey, J. W. Mink, M. N. Abdulla, C. E. Christoffersen, H. M. Gutierrez, P. L. Heron, C. W. Hicks, A. I. Khalil, U. A. Mughal, S. Nakazawa, T. W. Nuteson, J. Patwardhan, S. G. Skaggs, M. A. Summers, S. Wang, and A. B. Yakovlev, "Global modeling of spa-

tially distributed microwave and millimeter-wave systems," *IEEE Trans. Microwave Theory Tech.*, Vol. 47, pp. 830–839, June 1999.

[6] C. T. Tai, *Dyadic Green Functions in Electromagnetics*, IEEE Press, New York, New York, 1994.

[7] N. L. VandenBerg and P. B. Katehi, "Full-wave analysis of aperture coupled shielded microstrip lines," *IEEE MTT-S International Microwave Symposium Digest,* Vol.1, pp. 8–10, May 1990.

[8] C. W. Hicks, *Experimental and Electromagnetic Modeling of Waveguide-Based Spatial Power Combining Systems*, Ph.D. dissertation, North Carolina State University, Raleigh, NC, November 2002.

Chris W. Hicks received the B.S.degree in Electrical Engineering from the University of South Carolina, Columbia, in 1985, the M.S.E.E. degree from North Carolina A&T State University, Greensboro, in 1994, and the Ph.D. degree in Electrical Engineering from North Carolina State University, Raleigh, in 2002. In 1985, he joined the Naval Air Systems Command (NAVAIR), Patuxent River, MD, where he currently works for the RF Sensors Division as a Senior Engineer. His interests include electromagntic modeling of quasi-optical and spatial power combining systems, applied computational electromagnetics, and applications of microwave and millimeter-wave devices for radar, commumications, and electronic warfare applications.

Dr. Hicks was the recipient of two full-time training fellowships from NAVAIR. He is a member of the IEEE, Microwave Theory and Techniques society, and Antennas and Propagation society.

Alexander B. Yakovlev received the Ph.D. degree in Radiophysics from the Institute of Radiophysics and Electronics, National Academy of Sciences, Ukraine, in 1992, and the Ph.D. degree in Electrical Engineering from the University of Wisconsin at Milwaukee, in 1997. In summer of 2000, he joined the Department of Electrical Engineering, The University of Mississippi, University, as an Assistant Professor. His research interests include mathematical methods in applied electromagnetics, modeling of high-frequency interconnection structures and amplifier arrays for spatial and quasi-optical power combining, integrated-circuit elements and devices, theory of leaky waves, and singularity theory.

Dr. Yakovlev received the Young Scientist Award presented at the 1992 URSI International Symposium on Electromagnetic Theory, Sydney, Australia, and the Young Scientist Award at the 1996 International Symposium on Antennas and Propagation, Chiba, Japan. He is a Senior member of the IEEE and member of URSI Commission B.

Michael B. Steer received his B.E. and Ph.D. in Electrical Engineering from the University of Queensland, Brisbane, Australia, in 1976 and 1983, respectively. Currently he is Professor of Electrical and Computer Engineering at North Carolina State University. Professor Steer is a Fellow of the Institute of Electrical and Electronic Engineers for contributions to the computer aided engineering of non-linear microwave and millimeter-wave circuits. He is active in the Microwave Theory and Techniques (MTT) Society. In 1997 he was Secretary of the Society and from 1998 to 2000 was an Elected Member of its Administrative Committee. In 1999 and 2000 he was Professor in the School of Electronic and Electrical Engineering at the University of Leeds where he held the Chair in Microwave and Millimeter-wave Electronics. He was also Director of the Institute of Microwaves and Photonics at the University of Leeds. He has authored more than 240 publications on topics related to RF, microwave and millimeter-wave systems, to high speed digital design and to RF and microwave design methodology and circuit simulation. He is coauthor of the book *Foundations of Interconnect and Microstrip Design*, John Wiley, 2000. He is a 1987 Presidential Young Investigator (USA) and in 1994, and again in 1996, he was awarded the *Bronze Medallion* by U.S. Army Research for "Outstanding Scientific Accomplishment." He received the Alcoa Foundation Distinguished Research Award from North Carolina State University in 2003. Professor Steer is the Editor-In-Chief of the IEEE Transactions on Microwave Theory and Techniques (2003-2006).